Int. J. Solids Structures Vol. 21, No. 3, pp. 307–321, 1985
Printed in the U.S.A.

0020-7683/85 $3.00 + .00

A NONLINEAR CONSTITUTIVE MODEL FOR ICE†

W. SZYSZKOWSKI, S. DOST AND P. G. GLOCKNER
Department of Mechanical Engineering, The University of Calgary, Calgary, Alberta, Canada

(*Received* 10 *November* 1983)

Abstract—A six-parameter nonlinear model consisting of two springs and two dashpots is developed to represent the primary and secondary/steady creep stage of ice, the parameters of which are adjusted so as to obtain a creep function in agreement with experimental data and with standard creep rate expressions as given, for example, by Voitkovski[1]. The constitutive law for the model is derived in differential form and is applied to the time-deflection behaviour of imperfect simply-supported ice columns subjected to a constant axial load. The method of solution and step-by-step numerical integration technique introduced allows the use of the constitutive law in its 'exact' form. Results presented for a range of stress levels and temperatures indicate that such structures are inherently unstable and that the time to failure is very sensitive to these parameters.

1. INTRODUCTION

In dealing with the behaviour of various ice structures, the question arises as to whether it is possible to design a model which would simulate the time-dependent nonlinear behaviour of ice with sufficient accuracy, at least for a given constant temperature and within the primary and secondary/steady creep stages. Numerous experiments[1–6] indicate that the crystal structure as well as the mechanical properties of ice are significantly affected by its temperature and stress history as well as the meteorological and hydrodynamic conditions existing at the time of its formation. Therefore, river ice, for example, has properties quite different from those of sea or glacier ice.

Despite the variability in properties of ice, its mechanical behaviour can be approximated by viscoelastic material models. Thus, its instantaneous response to loads is elastic, followed by typical creep behaviour, including the primary (transient) creep, the secondary or steady creep, and the tertiary or accelerating creep stages. The analysis in this article is concerned with only the first two phases of creep behaviour of ice.

The creep behaviour of a material is normally specified by a so-called "creep-function" defining the creep rate under a constant stress level. There are numerous empirical or semi-empirical expressions for the creep function of ice, usually stated in a form

$$\frac{d\epsilon_{cr}}{dt} = \dot{\epsilon}_{cr} = B(\theta)[1 + f(t)]\sigma^n \tag{1}$$

in which $B(\theta)$ is a function of temperature, $f(t)$, a function of time defines the transient creep phase, σ denotes stress and n is a constant defining the 'nonlinearity' of the creep, with values ranging from 1.5–4.0. The model to be used in this study has a five-parameter creep function which is in agreement with that given in [1] and is expressed as

$$\dot{\epsilon}_{cr} = \frac{K}{3^{n+1/2}[1 + |\theta|]}\left[1 + \frac{mbt_0}{(1 + bt)^{m+1}}\right]\sigma^n \tag{2}$$

where the physical meaning of the various constants, b, K, m, n and t_0 and the characteristic features of eqn (2) are indicated on Fig. 1.

These features, which are to be incorporated into our spring-dashpot model, include

†The results presented here were obtained in the course of research sponsored by the Natural Sciences and Engineering Research Council of Canada in the form of a grant to the third author, Grant No. A-2736.

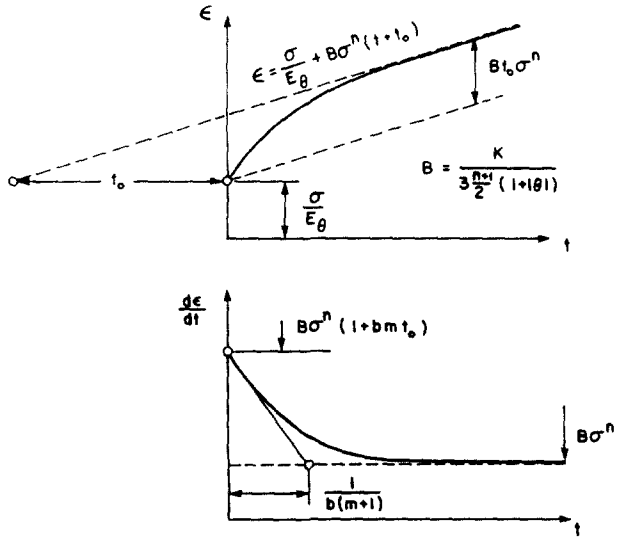

Fig. 1. Typical creep and creep-rate functions for ice.

(i) a purely elastic 'instantaneous' response, characterized by σ/E_θ, where E_θ is the sixth constant of the model;

(ii) a secondary, nonlinear elastic response, defined by $(Bt_0\sigma^n)$ which represents the elastic portion of the strain developed during the primary creep phase;

(iii) a maximum (initial) creep rate defined as $B\sigma^n(1 + bmt_0)$;

(iv) a minimum (steady) creep rate defined by $B\sigma^n$;

(v) an initial slope of the strain rate curve, defining the rate of creep decay and indicated by the slope intercept on Fig. 1 $(1/b(m + 1))$.

Experimental data suggests[1] that only E_θ and $B(\theta)$ are functions of the temperature.

After introducing the above outlined model and defining its parameters in agreement with experimental data for ice and with an expression given in [1], the model and its constitutive law, in 'exact' form, are used to analyse the time-deflection behaviour of a simply supported 'ice'-column with initial imperfections.

2. THE MODEL

Consider the viscoelastic model shown in Fig. 2 and consisting of a linear and a nonlinear spring, S_1 and S_2, respectively, as well as two nonlinear dashpots, D_1 and D_2. An analysis of the model indicates that its response is similar to that shown in Fig. 1. In particular, the linear spring S_1, defines the 'instantaneous' elasticity, given by

$$\sigma = \mathring{E}_1\epsilon_1'. \tag{3}$$

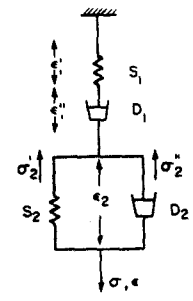

Fig. 2. Four-element model for ice.

The dashpot, D_1, describes the 'steady' creep rate, defined by

$$\sigma = \nu_1(\sigma) \frac{d\epsilon_1''}{dt} . \tag{4}$$

In order to conform with eqn (2), this relation is taken in the form

$$\sigma^n = \mathring{\nu}_1 \frac{d\epsilon_1''}{dt} , \tag{5}$$

where $\mathring{\nu}_1$ is a material constant. From a comparison of eqns (4) and (5), one obtains

$$\nu_1(\sigma) = \frac{\mathring{\nu}_1}{\sigma^{(n-1)}} . \tag{6}$$

The elements S_2 and D_2, responsible for the transient creep phase of the model, are defined as

For D_2

$$\sigma_2'' = \nu_2(\sigma_2'') \frac{d\epsilon_2}{dt} \tag{7a}$$

$$(\sigma_2'')^n = \mathring{\nu}_2 \frac{d\epsilon_2}{dt} \tag{7b}$$

$$\nu_2(\sigma_2'') = \frac{\mathring{\nu}_2}{(\sigma_2'')^{n-1}} \tag{7c}$$

For s_2

$$\mathring{E}_2\epsilon_2 = c\sigma_2' + (\sigma_2')^n \tag{8a}$$

or

$$\sigma_2' = E_2\epsilon_2, \tag{8b}$$

where

$$E_2 = \frac{\mathring{E}_2}{c + (\sigma_2')^{n-1}} , \tag{8c}$$

and where c was introduced to provide a finite stiffness to the unloaded spring S_2. Thus the model has been defined in terms of six parameters ($\mathring{E}_1$, $\mathring{E}_2$, c, $\mathring{\nu}_1$, $\mathring{\nu}_2$, n), which are to be related to the six parameters E_θ, B, b, m, n, t_0.

3. THE CONSTITUTIVE LAW FOR THE MODEL

The constitutive law for the model in differential form is derived using expressions (3)–(8), and standard procedures by writing

$$\sigma = \sigma_2' + \sigma_2'' \tag{9a}$$

$$\epsilon = \epsilon_1'' + \epsilon_1' + \epsilon_2 \tag{9b}$$

which, after simple transformations become

$$\frac{\sigma}{\nu_1}\left[1 + \frac{d}{dt}\left(\frac{\nu_2}{E_2}\right) + \frac{\nu_1\nu_2}{E_2}\frac{d}{dt}\left(\frac{1}{\nu_1}\right) + \nu_1\frac{d}{dt}\left(\frac{1}{E_2}\right)\right] + \frac{1}{E_1}\frac{d\sigma}{dt}\left[1 + \frac{d}{dt}\left(\frac{\nu_2}{E_2}\right) + \frac{E_1}{E_2}\left(1 + \frac{\nu_2}{\nu_1}\right)\right] - \frac{\nu_2}{E_2E_1}\frac{d^2\sigma}{dt^2} = \frac{d\epsilon}{dt}\left[1 + \frac{d}{dt}\left(\frac{\nu_2}{E_2}\right)\right] + \frac{\nu_2}{E_2}\frac{d^2\epsilon}{dt^2} . \tag{10}$$

For constant values of ν_1, ν_2 and E_2, this general constitutive law reduces to that of the four-element fluid material (see, for example [10]). Since, in our case, ν_1, ν_2, and E_2 are functions of the (internal) stresses σ_2' and σ_2'', these stress components should also be expressed in terms of σ and ϵ, including the history of loading, expressions which are derived

$$\sigma_2' = E_2\epsilon_2 = E_2\left[\epsilon - \frac{\sigma}{E_1} - \psi\right] \tag{11a}$$

$$\sigma_2'' = \sigma\left(1 + \frac{E_2}{E_1}\right) - E_2(\epsilon - \psi) \tag{11b}$$

where

$$\psi = \int_0^t \frac{\sigma(\tau)}{\nu_1(\tau)}\,d\tau. \tag{11c}$$

The creep rate for the model is given by

$$\frac{d\epsilon_{cr}}{dt} = \frac{d\epsilon_1''}{dt} + \frac{d\epsilon_2}{dt} = \frac{\sigma}{\nu_1} + \frac{\sigma_2''}{\nu_2} = \frac{\sigma}{\nu_2}\left(1 + \frac{E_2}{E_1} + \frac{\nu_2}{\nu_1}\right) - \frac{E_2}{\nu_2}(\epsilon - \psi). \tag{12}$$

The creep function for the model is obtained from eqn (10) by setting $\sigma = \sigma_0$ (as a result of which $\nu_1(\sigma) \to \nu_1(\sigma_0)$)

$$\frac{d^2\epsilon}{dt^2} + \frac{E_2}{\nu_2}\frac{d\epsilon}{dt}\left[1 + \frac{d}{dt}\left(\frac{\nu_2}{E_2}\right)\right] = \frac{\sigma_0}{\nu_1}\left[\frac{E_2}{\nu_2} + \frac{1}{\nu_2}\frac{d\nu_2}{dt} - \left(1 + \frac{\nu_1}{\nu_2}\right)\frac{1}{E_2}\frac{dE_2}{dt}\right] \tag{13}$$

the initial conditions for which, together with all constants and functions appearing in this expression are defined in the Appendix. Using a step-by-step integration procedure and a given set of values for the parameters $\mathring{E}_1$, $\mathring{E}_2$, c, $\mathring{\nu}_1$, $\mathring{\nu}_2$, n and the constant stress σ_0, eqn (13) can be solved numerically, subject to the initial conditions (eqns A1). The parameters are chosen so as to obtain the characteristic response indicated in Fig. 1 and to be in agreement with an expression for such creep behaviour given in [1].

Comparing the 'instantaneous' elastic stiffness, the secondary elasticity, maximum and minimum creep rates and the rate of decay of creep rate, one arrives at the following relations

$$\mathring{E}_1 = E_\theta \tag{14a}$$

$$\mathring{E}_2 = \frac{m + 1}{m + 1 - nm}\left(\frac{1}{Bt_0}\right) \tag{14b}$$

$$\mathring{\nu}_1 = 1/B \tag{15a}$$

$$\mathring{\nu}_2 = (Bbmt_0)^{-1} \tag{15b}$$

$$c = \frac{nm}{(m + 1 - nm)}\sigma_0^{n-1}. \tag{16}$$

4. NUMERICAL RESULTS FOR THE MODEL

To compare the creep function for the above defined model with that given in [1], eqn (13) was solved numerically using values for the various parameters as given in [1]

$$K = 2.59 \times 10^{-14} \frac{\text{deg}}{\text{hr(Pa)}^n}; \qquad E_\theta = 4[1 + 0.0125 \mid \theta \mid]\text{GPa}$$

$$n = 1.8; \qquad b = 0.5\ \text{hr}^{-1}$$

$$t_0 = 100\ \text{hr}; \qquad m = 1.0$$

$$\theta = -5°\text{C}.$$

The solution was carried out for two levels of stress, $\sigma_0 = 0.5$ MPa (see Fig. 3) and $\sigma_0 = 4.0$ MPa (see Fig. 4). A modified Euler method was used and in order to ensure satisfactory convergence, the time step, Δt, was limited to

$$\Delta t \leq \frac{0.1}{b(m + 1)}. \tag{17}$$

The results are depicted on Figs. (3) and (4) and indicate that the creep function for the model introduced here coincides with that given by Voitkovski[1]. Therefore, this model can be used to predict the behaviour of ice structures to the same degree of accuracy as is inherent in other empirical or semiempirical expressions available in the literature.

It may be noteworthy that the stiffnesses of the elements responsible for transient creep (S_2, D_2) are considerably smaller than those of the elements representing steady creep (S_1, D_1). For example, in the case of $\sigma_0 = 0.5$ MPa, $14.3 \leq E_1/E_2 \leq 15.8$, while

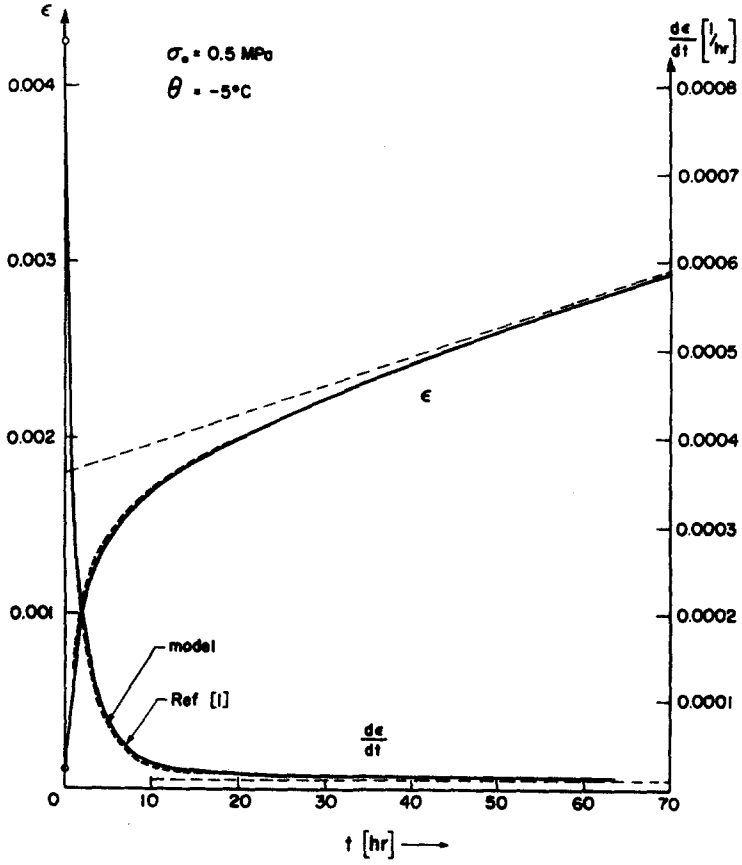

Fig. 3. Comparison of creep properties of model with those given in Ref. [1]—low stress level.

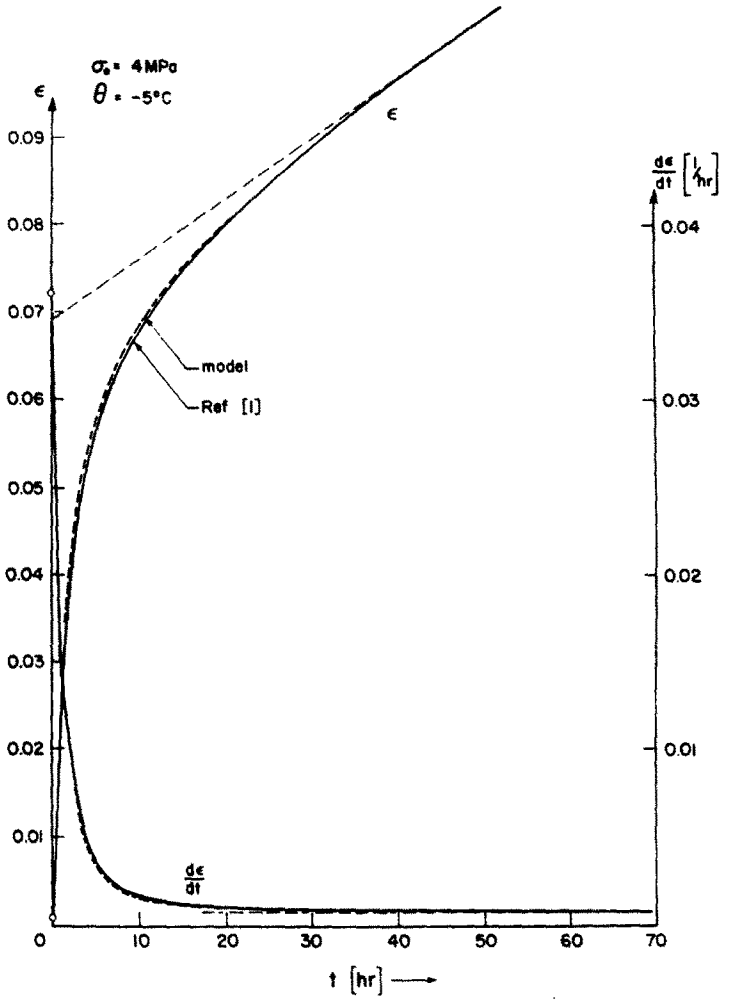

Fig. 4. Comparison of creep properties of model with those given in Ref. [1]—high stress level.

for $\sigma_0 = 4$ MPa, the same ratio becomes $75.3 \leq E_1/E_2 \leq 83.7$, the range being due to variation over time. The ratio of viscous constants is time and stress independent and is given by

$$\frac{\mathring{\nu}_1}{\mathring{\nu}_2} = bmt_0 = 50.$$

5. THE ICE COLUMN

Consider the simply-supoported column of length L, rectangular cross-sectional area A and with initial imperfection $w_0(x)$, shown in Fig. 5. The column is subjected to a constant force P. Note that the axial coordinate is denoted by x and the coordinate y is referenced to the current centroidal axis of the column. For creep rates ordinarily encountered in ice columns, quasi-static conditions are admissible (see [11]). Therefore, equations of equilibrium, as opposed to equations of motion, are written for the deformed column as

$$\left.\begin{aligned} \int_A \sigma(x, y, t)\, dA + P &= 0 \\ \int_A \sigma(x, y, t) y\, dA + P[w(x, t) + w_0(x)] &= 0 \end{aligned}\right\} \quad \text{for } t \geq 0. \tag{18, 19}$$

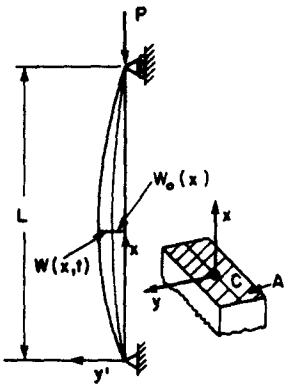

Fig. 5. Imperfect ice column geometry.

Differentiating without respect to time one obtains

$$\int_A (\mathrm{d}\sigma)\mathrm{d}A = 0 \tag{20}$$

$$\int_A (\mathrm{d}\sigma)y\,\mathrm{d}A + P(\mathrm{d}w) = 0 \tag{21}$$

in which

$$\mathrm{d}\sigma = \frac{\partial\sigma}{\partial t}\mathrm{d}t; \quad \text{and} \quad \mathrm{d}w = \frac{\partial w}{\partial t}\mathrm{d}t \tag{22}$$

are stress displacement increments corresponding to the time increment $\mathrm{d}t$.

Next, assume that the total strain rate is given as the sum of the viscous and elastic strain rates, expressed as

$$\frac{\mathrm{d}\epsilon}{\mathrm{d}t} = \frac{1}{E_\theta}\frac{\mathrm{d}\sigma}{\mathrm{d}t} + \frac{\mathrm{d}\epsilon_{cr}}{\mathrm{d}t}. \tag{23}$$

Thus we are saying that at every point of the structure, the stress and strain history possibly being different at such points, it is possible to divide the strain increment for every time interval ($\mathrm{d}t$) into an elastic and a viscous part. For the model introduced above, and using eqn (12), one obtains for the viscous portion of the strain rate the expression

$$\frac{\mathrm{d}\epsilon_{cr}}{\mathrm{d}t} = \frac{\sigma}{\nu_2}\left(1 + \frac{E_2}{E_2} + \frac{\nu_2}{\nu_1}\right) - \frac{E_2}{\nu_2}\left(\epsilon - \int_0^t \frac{\sigma(\tau)}{\nu_1(\tau)}\,\mathrm{d}\tau\right), \tag{24}$$

which allows the determination of the viscous part of the strain increment provided the strain at a given time and the stress history is known.

Using the Bernoulli-Euler hypothesis, the total strain increment in a fibre at a distance y from the centroid of the cross-section is given by

$$\mathrm{d}\epsilon(x, y, t) = \mathrm{d}\epsilon_0(x, t) - y\mathrm{d}\kappa(x, t), \tag{25}$$

in which $\mathrm{d}\epsilon_0(x, t)$ denotes the axial strain increment and $\mathrm{d}\kappa = \partial\kappa/\partial t\,\mathrm{d}t$, is the curvature increment of the centroidal axis.

From eqns (23) and (25), one obtains the stress increment in the form

$$\mathrm{d}\sigma(x, y, t) = E_\theta[\mathrm{d}\epsilon_0(x, t) - y\mathrm{d}\kappa(x, t) - \mathrm{d}\epsilon_{cr}(x, y, t)]. \tag{26}$$

Substituting eqn (26) into eqn (20) one obtains

$$d\epsilon_0(x, t) = \frac{1}{A}\int_A d\epsilon_{cr} dA \tag{27}$$

while from eqn (26) and eqn (21) we have

$$-E_\theta I d\kappa + P dw = E_\theta \int_A (d\epsilon_{cr}) y dA \tag{28}$$

where I denotes the moment of inertia of the column cross-section. We assume also that the change in curvature during the time interval dt is small enough so as to permit linearization and to write

$$d\kappa = (\kappa)_{t+dt} - (\kappa)_t = -\frac{d^2}{dx^2}(dw) \tag{29}$$

which, when substituted into eqn (28), results in

$$E_\theta I \frac{d^2}{dx^2}(dw) + P dw = E_\theta \int_A (d\epsilon_{cr}) y dA. \tag{30}$$

Equations (27) and (30) thus allow determination of the axial strain increment and the lateral displacement increment during the time interval dt, knowing only the viscous creep increment at each point of the column. The total strain, stress and additional deflection are obtained by simple summation of increments for these variables. For details, see, for example [12].

6. NUMERICAL PROCEDURE AND RESULTS

The column is divided into M equal segments of length $\Delta x = L/M$ while the cross-section is split into M equal layers of thickness $\Delta y = h/M$ (see Fig. 6). At each point, with coordinates x_i and y_j, the increment values $(d\epsilon_{cr})_{ij}$, $d\epsilon_{ij}$, $d\sigma_{ij}$, $(d\epsilon_0)_i$ and dw_i are evaluated for the time increment, dt, and then the equations of equilibrium are verified at each node point, x_i, using

$$\left|\frac{1}{P}\int_A \sigma(x_i, y, t)\, dA + 1\right| \leq \delta \qquad i = 1, 2 \ldots M + 1 \tag{31}$$

$$\left|\frac{1}{P\left[w\left(\frac{L}{2}, t\right) + w_0\left(\frac{L}{2}\right)\right]}\int_A \sigma(x_i, y\ t) y\, dA + \frac{[w(x_i, t) + w_0(x_i)]}{\left[w\left(\frac{L}{2}, t\right) + w_0\left(\frac{L}{2}\right)\right]}\right| \leq \delta \qquad i = 1, 2 \ldots M + 1 \tag{32}$$

in which δ is an arbitrarily small positive number. In order to obtain the desired accuracy, the time interval, dt, is decreased. Details of the integration procedure used are given in [11].

The numerical results indicate that the choice for the time interval, dt, to ensure rapid convergence and the desired accuracy, depends only on the material model and its parameters, and is independent of the loading and the column geometry, including slenderness and imperfection. Thus, for a proper simulation of the behaviour of an ice column, the time interval chosen must meet the criterion given by eqn (17). This is, in

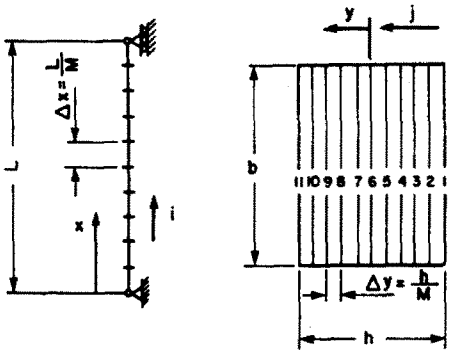

Fig. 6. Discretization of ice column.

some sense, unfortunate since it puts a limit on the magnitude of the time interval, which in the case of low loads and corresponding low creep rates results in an uneconomical solution procedure in terms of computer time.

The values for the ice parameters used in this analysis are those used in Section 4 for the model.

Typical results for the behaviour of such an imperfect ice column are indicated in Fig. 7. The time-deflection curve is a monotonically increasing function of time indicating that such structures are inherently unstable with displacements unbounded. The rate of deflection seems to increase rapidly when the midspan displacement becomes approximately equal to the width of the column, h, with a concentration of deformation at midspan creating what may be referred to as a "viscous hinge". Since such accelerated deformations and deflections are potentially dangerous, the time at which such a hinge begins to form is referred to as the critical time, t_{cr}, and is established as the time for which the total lateral midspan displacement reaches a value h. The "acceleration" in strain can also be observed in the stress-strain history diagram given in

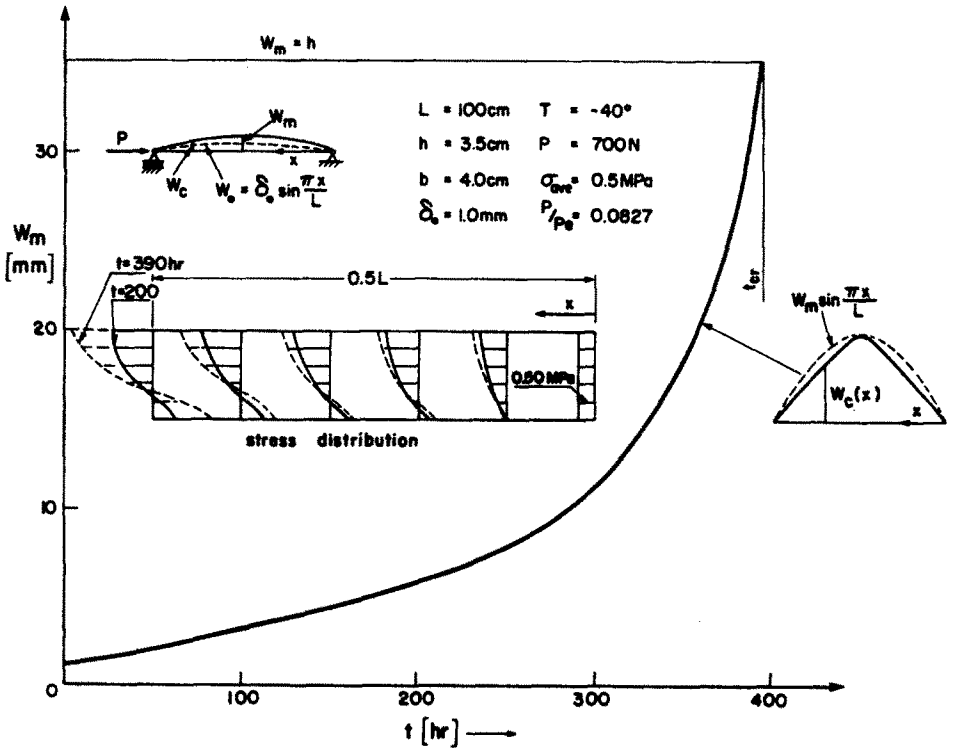

Fig. 7. Typical time-delfection plot of imperfect ice column.

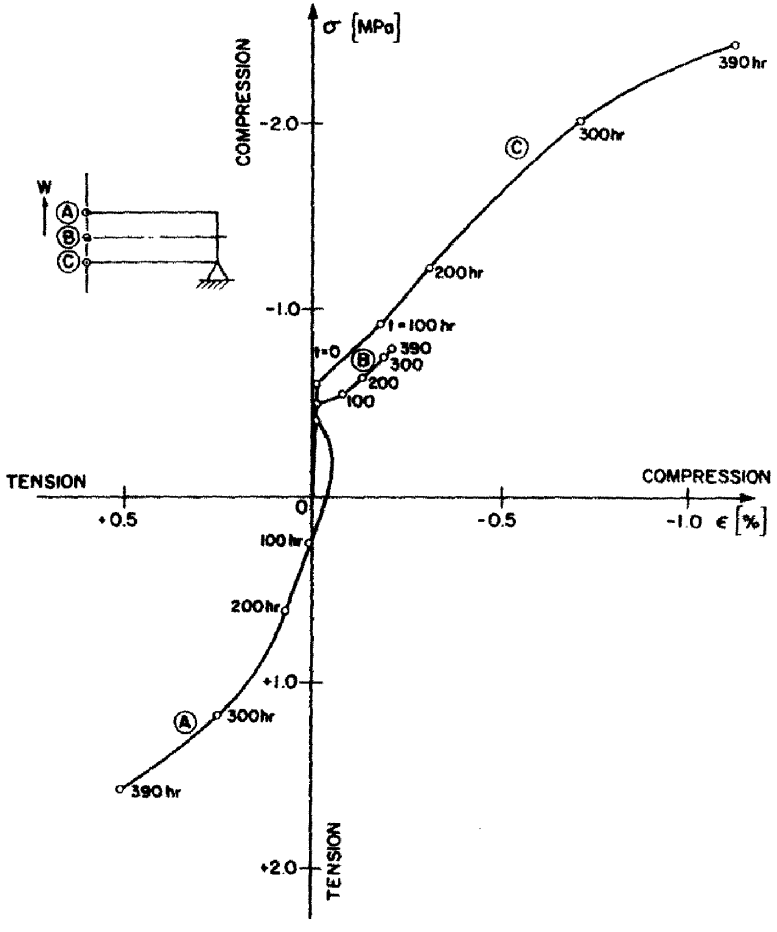

Fig. 8. Stress-strain history at selected points.

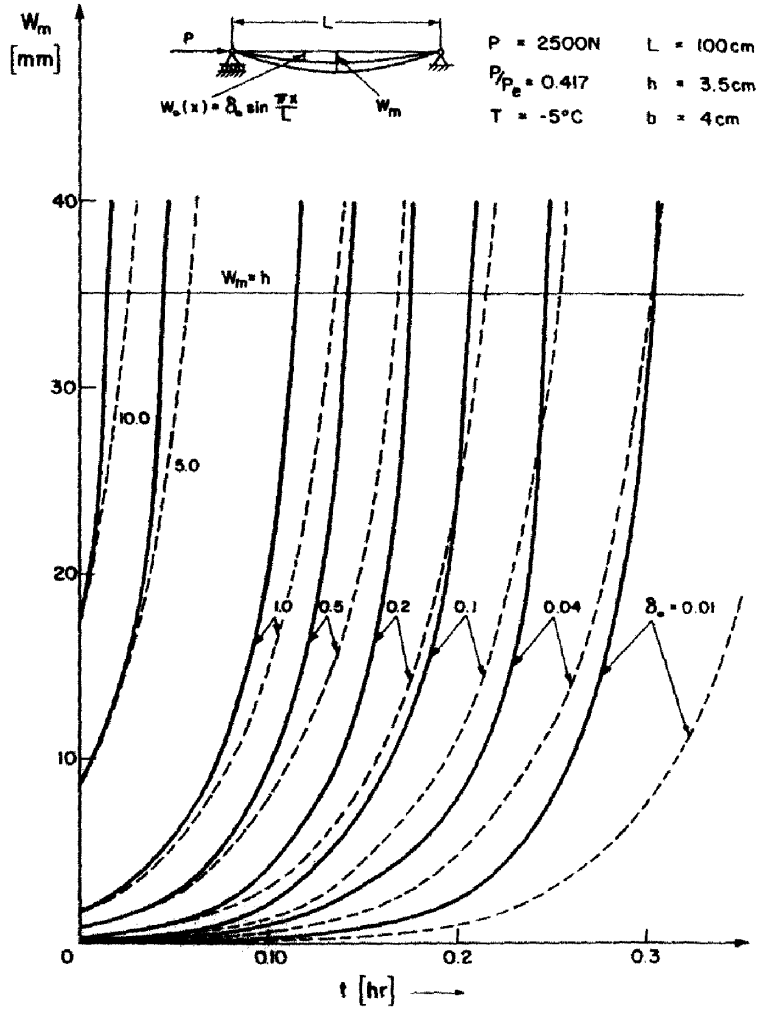

Fig. 9. Effect of initial imperfection magnitude on the time-delfection behaviour of ice columns—$T = -5°C$.

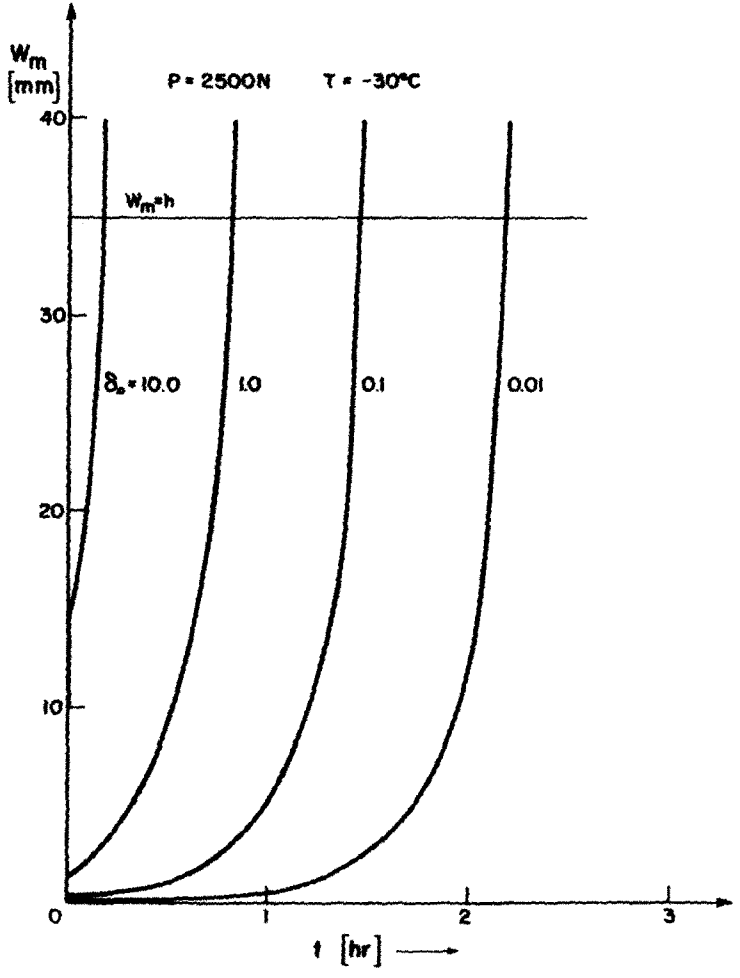

Fig. 10. Effect of initial imperfection magnitude on the time-delfection behaviour of ice columns—$T = -30°C$.

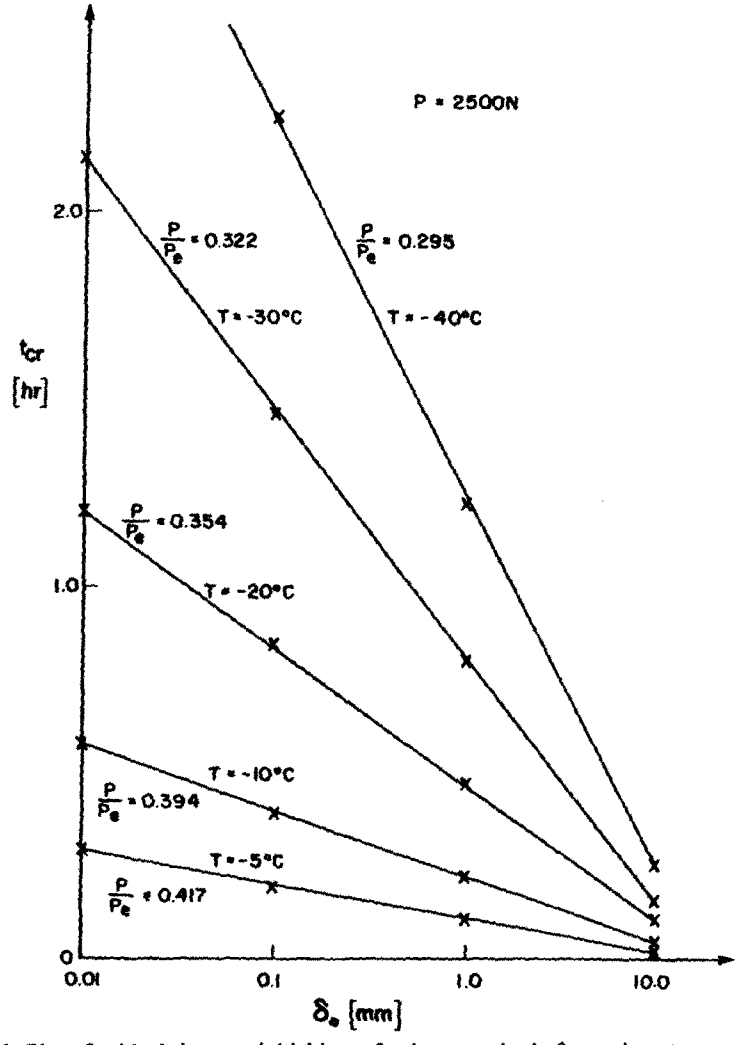

Fig. 11. Plot of critical time vs. initial imperfection magnitude for various temperatures.

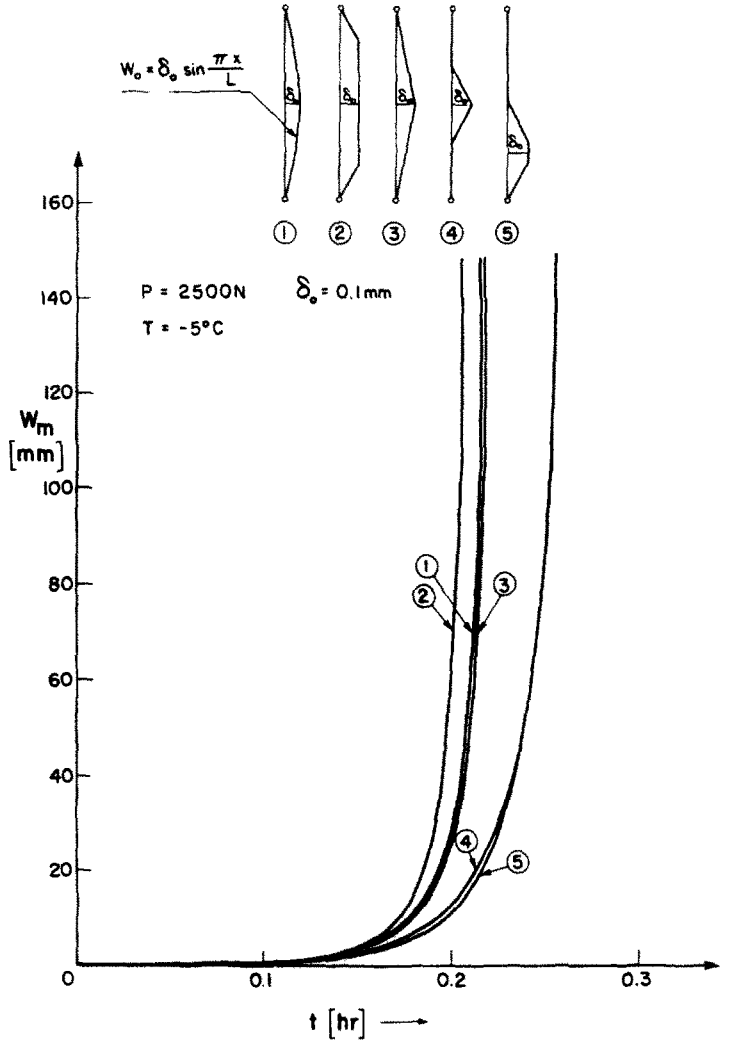

Fig. 12. Effect of initial imperfection shape on the time-deflection behaviour of ice columns.

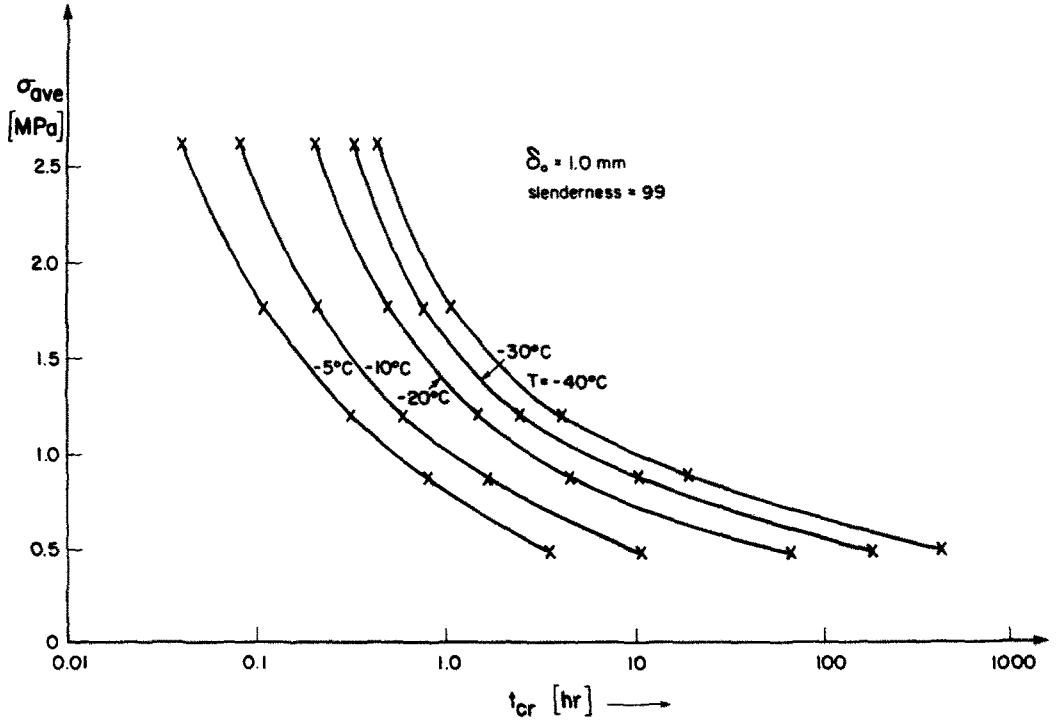

Fig. 13. Plot of average stress vs. critical time for various temperatures.

Fig. 8. Similar behaviour was obtained for other column geometries. and for a range of loads and temperatures.

Fig. 9 gives results on the effect of initial imperfections. For a comparison, predicted column behaviour using an approximate solution technique given in [12] is also indicated on the figure by means of dotted lines. In that solution technique, instead of eqn (12), the creep rate is taken to be given by eqn (2) which is valid only for constant stress. Consequently, the rate of deformation is smaller and the difference between the approximate solution and our results increases with increasing critical time, indicating that such an approximation in the constitutive law and its associated solution technique[12] leads to results which are nonconservative.

Results from a similar analysis, with only the temperature being changed from $-5°C$ to $-30°C$, are given in Fig. 10, in which the corresponding predicted column behaviour, based on the approximation discused above, are not included.

Results for critical times from such analyses are plotted on Fig. 11 as a function of initial imperfections and for various constant temperatures. It is interesting to note that such results, plotted on a semi-log scale, can be approximated by straight lines for a given temperature.

The influence on the column behaviour of the type of imperfection is indicated in Fig. 12, where results for various imperfections are compared with the standard 'sinusoidal' initial deflection shape. The curves in this figure show that column behaviour depends primarily on the first harmonic of the Fourier series expansion for the initial

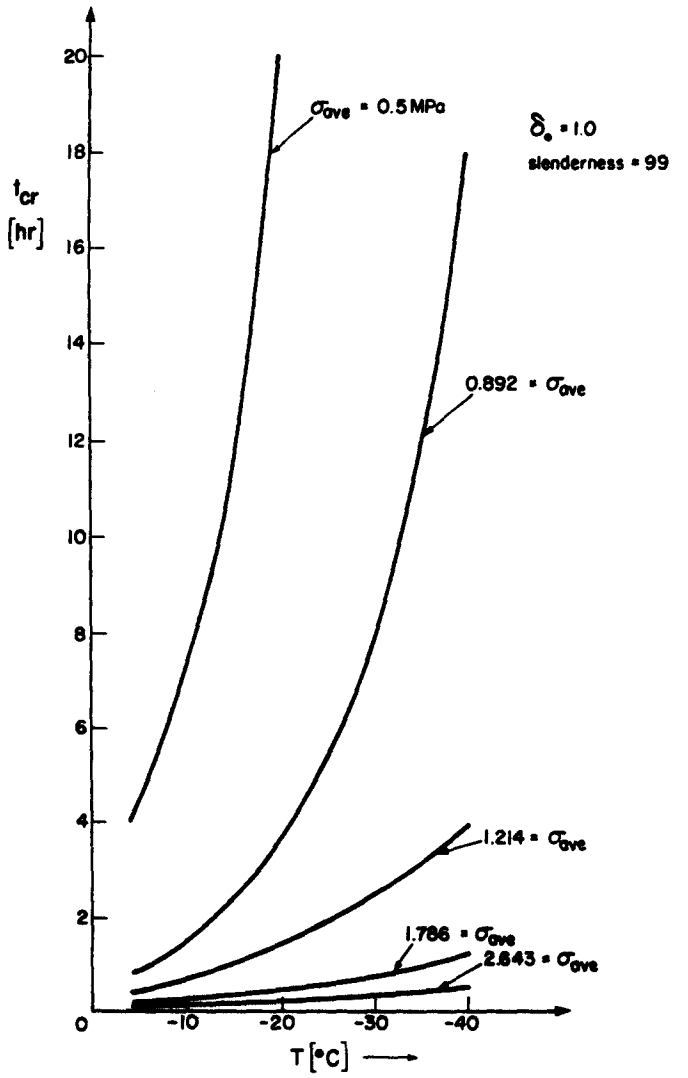

Fig. 14. Variation of critical time with temperature for various stress levels.

imperfection. The shapes for cases 4 and 5 (in Fig. 12) were chosen so that the first harmonics were identical.

Figure 13 shows the variation of average stress, $\sigma_{ave.}$ vs. critical time for various temperatures. These results underline the significant influence of temperature on the behaviour of such ice columns.

The final figure (Fig. 14) indicates the relationship between critical time and temperature, for various constant average stress levels. The extreme sensitivity of the column behaviour to stress level is clearly indicated by the curves shown on this diagram.

CONCLUSIONS

Taking the expression given in [1] as representative of ice behaviour, a six-parameter nonlinear model, consisting of two springs and two dashpots is introduced to simulate the thermo-mechanical properties of ice. The constitutive law for the model is derived in differential form and the values of the model parameters are expressed in terms of the parameters of Voitkovski's formula by comparing, respectively, characteristic features, including "instantaneous" stiffness (elasticity), 'secondary' elasticity, maximum and minimum creep rates and rate of decay of creep rate. It is shown that the creep function for the model introduced here coincides with that given in [1] in the transient and steady phases of creep. Thus this model is an appropriate simulation for ice behaviour, at least within the accuracy afforded by other models and/or empirical and semi-empirical expressions known to the authors to be available in the literature.

A characteristic feature of the model is the considerably smaller stiffness of the elements responsible for the transient phase of the creep as compared to those which represent the steady creep. Therefore, the behaviour of the column is most significantly influenced by the primary/transient phase, an influence which also greatly affects the numerical treatment of the problem.

The numerical integration procedure adopted made it possible to utilize the constitutive law in its 'exact' form taking into account all viscoelastic properties inherent in the model.

The numerical results presented indicate that the time interval appropriate for rapid convergence and acceptable accuracy is a function only of the model parameters and is independent of the load and the geometry of the column. This is, of course, a direct result of the Voitkovski model, suggesting that the period of transient creep is independent of stress level and temperature.

The results from the analysis of the imperfect ice columns show that such structures undergo lateral deflections which are monotonically increasing functions of time, rendering such columns inherently unstable. When the midspan deflection reaches a magnitude approximately equal to the width of the column, a kind of hinge, referred to as a 'viscous hinge', develops at which deformation and curvature changes are concentrated. The development of this hinge contributes to the acceleration of the column deflections, leading to large displacements and/or collapse. Therefore, the time associated with the initiation of this hinge formation, which corresponds to a total lateral deflection approximately equal to the width, h, of the column, is defined in this study as the 'critical' time, t_{cr}. This time is shown to be a function of stress level, temperature and shape and value of initial imperfections. The results indicate the extreme sensitivity of the imperfect ice column behaviour to stress level and temperature.

REFERENCES

1. K. F. Voitkovski, The Mechanical Properties of Ice, Izd. Akademii Nauk SSSR, 1960, *Trans. AMS-T-R*-391, *Am. Met. Soc.*, Office of Tech. Services, U.S. Dept. of Commerce, Washington, p. 25.
2. B. Michel, *Ice Mechanics*, Les Presses de L'Universite Laval, Quebec (1978).
3. P. V. Hobbs, *Ice Physics*, Clavendon Press, Oxford (1974).
4. W. F. Weeks and M. Mellor, *Mechanical Properties of Ice in the Arctic Seas*, Arctic Technology and Policy, MIT Press, March (1983).
5. R. G. Stanley and P. G. Glockner, The use of reinforced ice in constructing temporary enclosures, *Marine Sci. Comm.* 1(6) (1975).
6. P. G. Glockner, *Reinforced ice domes: igloos of the 21st century?*, Dept. Mech. Engng, The University of Calgary, Report No. 203, June (1981).

7. Y. P. Doronin and D. E. Heysin, *Sea Ice* (in Russian), Hydrometeoizd, Leningrad (1974).
8. P. Barnes and J. C. F. Walker, The friction and creep of polycrystalline ice, *Proc. R. Soc.*, A324 (1971).
9. M. Mellor and D. M. Cole, Stress-strain-time relation for ice under uniaxial compression, *Cold Region Sci. Tech.*, Vol. 5 (1983).
10. W. Flugge, *Viscoelasticity*, Blaisdell Pub. Comp. (1967).
11. W. Szyszkowski and P. G. Glockner, *The imperfect linearly viscoelastic column*, Dept. of Mech. Engng, The University of Calgary, Report No. 271.
12. T. H. Lin, Creep deflections and stresses of beam-columns, *J. Appl. Mech.* 25(1) (1958).

APPENDIX

The initial conditions for eqn (13) are given as at $t = 0$:

$$\epsilon = \epsilon_0 = \frac{\sigma_0}{E_1} \tag{A1a}$$

$$\psi = 0 \tag{A1b}$$

$$\sigma_2'' = \sigma_0 \tag{A1c}$$

$$\nu_2 = \frac{\dot{\nu}_2}{\sigma_0''^{-1}} \tag{A1d}$$

$$\frac{d\epsilon}{dt} = \frac{\sigma_0}{\nu_1} + \frac{\sigma_2''}{\nu_2} = \frac{\sigma_0''}{\dot{\nu}_1}\left(1 + \frac{\dot{\nu}_1}{\dot{\nu}_2}\right) \tag{A1e}$$

$$E_2 = \frac{\dot{E}_2}{c} \tag{A1f}$$

$$\frac{d\sigma_2''}{dt} = -\frac{\dot{E}_2}{c}\frac{\sigma_0''}{\dot{\nu}_2} \tag{A1g}$$

$$\frac{d\nu_2}{dt} = (n-1)\frac{\dot{E}_2}{c} \tag{A1h}$$

$$\frac{dE_2}{dt} = 0. \tag{A1i}$$

The constants and functions appearing in these equations and in eqn (13) are defined by

$$\nu_1 = \frac{\dot{\nu}_1}{\sigma_0''^{-1}} = \text{constant} \tag{A2a}$$

$$\psi = \int_0^t \frac{\sigma_0''\, d\tau}{\dot{\nu}_1} = \frac{\sigma_0''}{\dot{\nu}_1} t \tag{A2b}$$

$$\sigma_2'' = \sigma_0\left(1 + \frac{E_2}{E_1}\right) - E_2\left(\epsilon - \frac{\sigma_0''}{\dot{\nu}_1} t\right) \tag{A2c}$$

$$E_2 = \frac{\dot{E}_2}{c + (\sigma_0 - \sigma_2'')^{n-1}} \tag{A2d}$$

$$\nu_2 = \frac{\dot{\nu}_2}{(\sigma_2'')^{n-1}} \tag{A2e}$$

$$\frac{d\nu_2}{dt} = -\dot{\nu}_2 \frac{n-1}{(\sigma_2'')^n}\frac{d\sigma_2''}{dt} \tag{A2f}$$

$$\frac{d\sigma_2''}{dt} = -\frac{\dfrac{\dot{E}_2}{c + (\sigma_0 - \sigma_2'')^{n-1}}\left(\dfrac{d\epsilon}{dt} - \dfrac{\sigma_0''}{\nu_1}\right)}{1 - \dfrac{(n-1)(\sigma_0 - \sigma_2'')^{n-1}\dot{E}_2}{[c + (\sigma_0 - \sigma_2)^{n-1}]^2}\left(\dfrac{\sigma_0}{E_1} - \epsilon + \dfrac{\sigma_0''}{\dot{\nu}_1} t\right)} \tag{A2g}$$

$$\frac{dE_2}{dt} = (n-1)\dot{E}_2 \frac{(\sigma_0 - \sigma_2'')^{n-2}}{[c + (\sigma_0 - \sigma_2)^{n-1}]^2}\frac{d\sigma_2''}{dt}. \tag{A2h}$$